2024 IEEE International Conference on Robotics and Automation (ICRA 2024)
May 13-17, 2024. Yokohama, Japan

WAVE: An open-source underWater Arm-Vehicle Emulator

Marcus Rosette[1], Hannah Kolano[1], Chris Holm[1],
Geoffrey A. Hollinger[1], Aaron Marburg[2], Madison Pickett[2], Joseph R. Davidson[1]

***Abstract*— Underwater vehicle manipulator systems (UVMS) are increasingly popular platforms for performing subsea operations that require precision manipulation. While there is high demand for fully autonomous or even semi-autonomous systems, most UVMS still require human support teams. Developing new hardware and algorithms for autonomous underwater manipulation is challenging. Simulations do not capture the full complexity of the underwater environment, and deploying a UVMS at sea for testing/validation is resource-intensive and expensive. In this paper, we present a physical testbed for underwater manipulation that bridges the gap between simulation and full field trials. The underWater Arm-Vehicle Emulator (WAVE) is a 10-degree of freedom system designed to replicate an inspection-class UVMS. WAVE includes an underwater perception sensor and has 2 operating modes: rigid or passive-mode. In passive-mode, the ROV body can pitch similar to how a dynamically-coupled underactuated UVMS without pitch control would rotate during manipulation tasks. To validate the overall design and passive pitch concept, we evaluated the testbed during underwater experiments in energetic conditions at a wave basin. To support continued research and development in underwater robotics, we make the design open-access and freely available to the community.**

I. Introduction

Underwater vehicle manipulator systems (UVMS) play an increasingly important role in subsea applications such as infrastructure maintenance (e.g., of underwater cables, wave energy converters, etc.), environmental monitoring, and scientific sampling and exploration [1]. While there is strong demand to deploy semi-autonomous robots that minimize the workload of human operators, most UVMS still require continuous operator control, and often the support of a team of human operators and support staff during operations [2]. This is especially true during activities that require dexterous manipulation. The unstructured underwater environment is extremely challenging: turbid water can degrade perception capabilities, Global Navigation Satellite System (GNSS) is unavailable for localization, communications and data bandwidth are constrained, and the increased dynamic complexity from energetic currents and waves make planning and control difficult.

Research supported in part by ONR/NAVSEA contract N00024-10-D6318/DO# N0002420F8705 (Task 2: Fundamental Research in Autonomous Subsea Robotic Manipulation) and ONR grant N00014-21-1-2052.

[1]Collaborative Robotics and Intelligent Systems (CoRIS) Institute, Oregon State University, Corvallis OR 97331, USA {rosettem, kolanoh, christopher.holm, geoff.hollinger, joseph.davidson}@oregonstate.edu

[2]Applied Physics Laboratory, University of Washington, Seattle WA 98105, USA {amarburg,mpick}@uw.edu

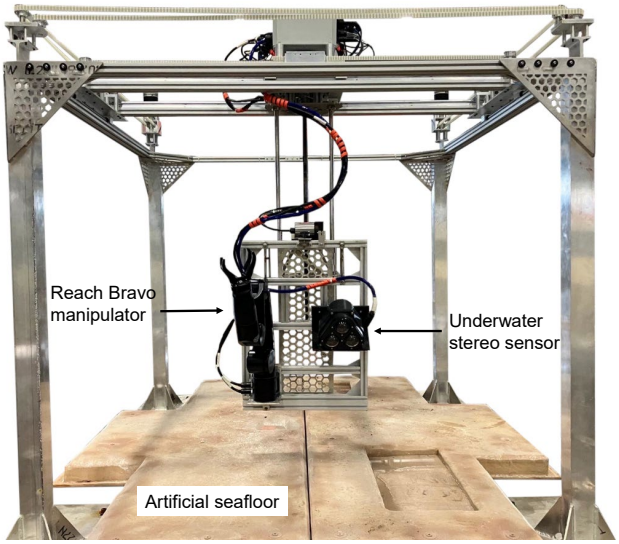

Fig. 1: The WAVE testbed includes a waterproof stereovision sensor and Reach Robotics (Sydney, Australia) underwater Bravo manipulator mounted to a 4-degree of freedom gantry system. If desired, the vertical column can be made passively compliant such that the manipulator and sensor pitch in energetic environments.

In addition to the technical challenges of the underwater environment, there are also logistical constraints that can impede research and development (R&D) in underwater robotics. Operating a UVMS at sea is resource-intensive, high-risk, and expensive. Additionally, it is difficult to collect the ground truth information (e.g. vehicle position, georeferenced point clouds, etc.) needed to evaluate and validate algorithms. While simulation environments can provide this ground truth, they do not sufficiently capture the complexities of the real world environment such as time-varying water turbidity and realistic energetic dynamics. Likewise, computational algorithms that work in simulation may not be deployable on a UVMS due to bandwidth constraints.

One way to support R&D year-round and help bridge the gap between simulation and full field deployments at sea is with a realistic testbed, i.e. *a physical twin*. In this paper, we present WAVE: an underWater Arm-Vehicle Emulator, a novel physical testbed developed for underwater manipulation studies. Shown in Fig. 1, the testbed is a 10-degree of freedom (DOF) kinematically redundant system consisting of a 4-DOF positioning gantry carrying a 6-DOF electric subsea manipulator and stereovision sensor. WAVE provides the following capabilities:

- **Replicated remotely operated vehicle (ROV) motion:** surge-sway-heave-yaw within an approximately 2 m x

2 m x 1 m square workspace

- **Ground truth localization:** feedback from joint encoders at each axis can be used to accurately reconstruct the forward kinematics of the testbed and provide accurate state estimation
- **Rigid or passively compliant operating modes:** in the passive-mode, the ROV body can pitch similar to how a dynamically-coupled underactuated UVMS without pitch control would rotate during manipulation tasks
- **Modularity:** the testbed can be disassembled and reassembled within two hours

To accurately replicate dynamic coupling in the passively compliant mode, we developed a rigid body model of an idealized UVMS and then used simulation results to create a compliant, linear pitch mechanism. We validated the testbed concept with underwater experiments in an energetic environment at the O.H. Hinsdale Wave Research Laboratory (Corvallis, OR, USA). The primary benefit of WAVE is that it enables more realistic experiments in lab-based environments (e.g. human user studies, evaluation of grasp planning algorithms, whole body control development, etc.). To support continued research in underwater manipulation, we have also made the testbed design open-source and freely available.

II. Prior Work

A. Underwater Simulators

There has been substantial prior work on the development of simulators for terrestrial and underwater robotics [3], [4]. For lightweight underwater vehicles where the manipulator has considerable inertia compared to the vehicle (a floating base), it is important to model dynamic coupling since reaction forces and torques that occur during manipulation tasks can affect the stability of the vehicle [5]–[7]. One of the more well-known simulators is UUV Simulator [8]. While UUV Simulator does model hydrodynamic, hydrostatic forces, and a portion of dynamic coupling in the rigid-body model of the vehicle, fully modeling the coupling is challenging due to constraints in the default form of the rigid-body equation of motion in the underlying physics engine. A more recent underwater robotics simulator is HoloOcean [9], an open-source platform that is actively maintained. Built upon a game engine that provides simulation dynamics and realistic graphics, its main focus is multiagent support, implementations of common underwater sensors, and simulated communications support. While simulation-based modeling can reconstruct a portion of the dynamics imposed on a UVMS, they are not yet mature enough to capture all physical disturbances or interaction forces that are present in a real hydrodynamic environment [10].

B. Robotic Testbeds

The use of testbeds/physical twins as research development platforms has seen adoption in multiple domains such as agriculture (where annual seasonal constraints often limit the time available for data collection and testing), multi-robot coordination [11], and unmanned aerial vehicles [12]. Velasquez et al. [13] built a physical orchard proxy that replicated the mechanics of apple picking and used it to train a grasp classifier. They showed that a classifier trained on the proxy performed as well in the orchard as a classifier trained on real data. Similarly, Junge et al. [14] trained a robotic raspberry harvester in the lab using a sensorized physical simulator of a raspberry plant; the system achieved 80% success in the field without any modifications to the lab-trained robot.

There have also been several testbeds built for underwater manipulation studies [15]. Cetin et al. [10] built a UVMS emulator with a Stewart Platform and industrial manipulator. Designed for underwater control studies in a dry lab environment, the emulator used input motion data captured from a deployed ROV. The testbed did not include any perception hardware. Researchers at the University of Girona rigidly mounted their ROV to a fixed aluminum frame in order to test panel manipulation algorithms [16], and NASA's Jet Propulsion Laboratory mounted their prototype arm to a fixed frame for similar testing [17]. The University of Girona's setup requires an expensive ROV as a prerequisite, but crucially, neither allows for ROV motion to be considered or replicated. One of the most comprehensive testbeds was built by the German Research Center for Artificial Intelligence (DFKI) in Bremen. They built a large UVMS testing facility that integrated an overhead 3-axis gantry crane with a hydraulic manipulator in a water basin [18]. The facility was designed to replicate a work class ROV with an assumed vehicle mass of 3290kg in water, an expensive system inaccessible to most academic researchers. We focus instead on an inspection class UVMS as the embodied system for our testbed.

III. Methods

The WAVE testbed (see Fig. 2 (*left*)) is designed to emulate motions of common 4-DOF inspection class ROVs. With the addition of a 6-DOF manipulator and stereo perception sensor, the testbed has the motion and perception capabilities similar to a UVMS. Sections III-A and III-B describe, respectively, the testbed's mechanical design and underwater camera. To replicate the dynamic coupling between the manipulator and vehicle, we developed a hydrodynamic model (Sec. III-D) and used simulation to drive integration of passive pitch compliance. The design presented here is modeled after the Falcon ROV (Saab Seaeye, Hampshire, UK), but could be easily modified for other ROVs by changing modeling parameters. We present our experimental setup for validating the testbed in Sec. III-E.

A. Mechanical and Electrical Design

The testbed has 4 actuated DOF: 3 translational directions (X-Y-Z) and 1 rotational axis (Yaw). Each axis is actuated with a ClearPath integrated servo motor (Teknic, Victor, NY, USA). To generate motion in the XY-plane, the testbed uses a Core-XY belt/pulley transmission system to drive a central carriage along linear rails. With the Core-XY system, individual actuator motion (i.e. one servo rotating and one servo fixed) generates diagonal carriage movement and paired actuation generates coordinated "left", "right", "forward", or

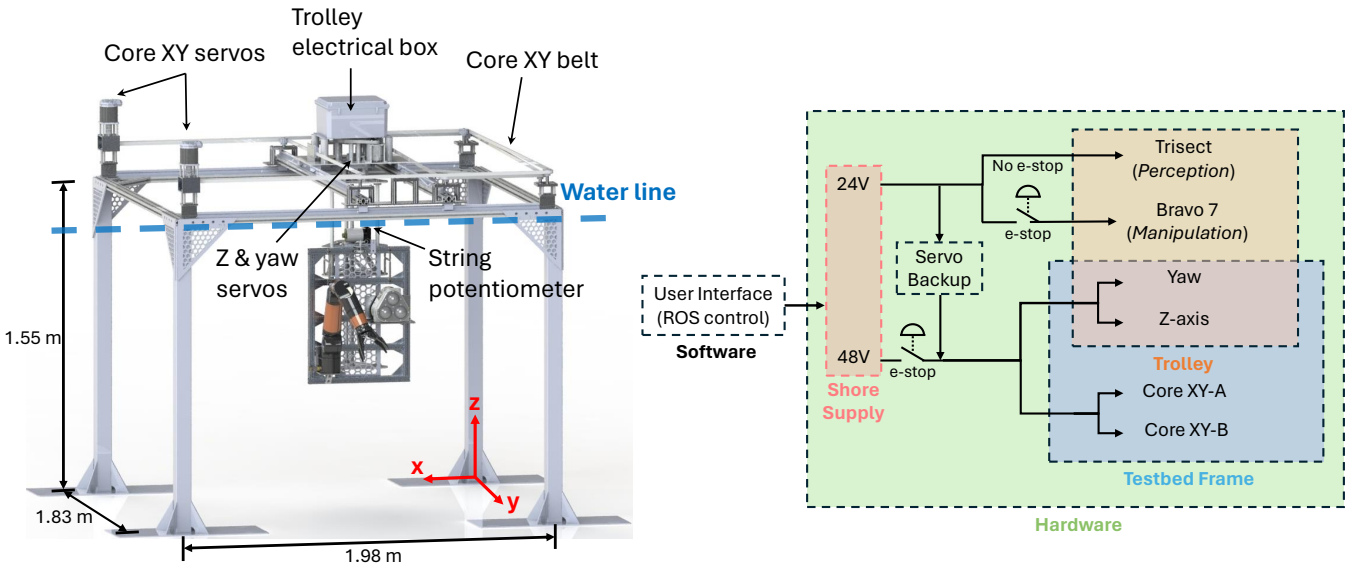

Fig. 2: *Left*: CAD rendering of WAVE. A belt & pulley system drive the central carriage in the XY plane. *Right*: System components; all components require either 24V or 48V power.

"backward" movements. Compared to a traditional gantry design, the Core-XY system allows the larger X-Y actuators to remain fixed to the frame, reducing the mass of the moving carriage. The XY frame is mounted to 4 welded square aluminum legs with slotted feet for anchoring to the floor; the testbed's overall dimension is 1.95 m x 1.83 m x 1.55 m.

The mobile trolley carriage includes an electrical junction box, the Yaw and Z-axes, and a suspended aluminum frame with the underwater manipulator and perception sensor (Fig. 2). The Yaw and Z-axes are housed in the vertical column mounted to the Core-XY motion stage through a slewing ring. The Yaw servo rotates the slewing ring through a 5:1 pulley system, which in turn rotates the vertical column. Within this column is the Z-axis servo, which drives the Z motion stage (with the manipulator and perception sensor) using a leadscrew, with a total travel length of 0.75 m. The actuator integrates with the leadscrew via a 5:1 planetary gearbox and flexible coupling to ensure smooth motion of heavy payloads attached to this motion stage. The underwater manipulator is an all-electric 6-DOF Bravo manipulator from Reach Robotics (Sydney, Australia), with a 1-DOF gripper [19].

To enable passive compliance in the pitch axis, the suspended aluminum frame has hinges mounted at its base along with a pair of extension springs mounted at its top (Fig. 6). With varying external forces (i.e. energetic environments, manipulator motions, or end-effector payloads), the extension springs are engaged and the frame passively pitches, pivoting about its base. Section III-D describes the analysis used to select the spring stiffness. If passive compliance is not desired (e.g. ground truth kinematics are required for collecting data with the perception sensor), the pitching frame can be rigidly locked with a pin.

The Clearpath servos are controlled via a multi-drop serial bus. In parallel, the WAVE testbed provides ethernet to interface with the manipulator and perception sensor. As shown in Fig. 2 (*right*), perception and manipulation are powered with 24V while all servos are powered with 48V and a backup 24V to maintain encoder position data if the 48V is terminated. Conventional (non-waterproofed) cables extend from shore to the trolley box; waterproof power and signal cables then pass from the trolley box to the Bravo manipulator and perception sensor. All components located below the z-axis actuator are designed for continuous submersion (e.g., stainless steel or anodized aluminum). All WAVE assembly documentation (e.g CAD, bill of materials, etc.) are freely available.[1]

B. Perception Sensor

All WAVE testing thus far has used the Trisect perception head developed by the University of Washington - Applied Physics Laboratory (UW-APL). Trisect was designed as an accessible, open source sensor for underwater stereo vision and perception research using commercial-off-the-shelf parts (Figure 3)[2]. Trisect includes a stereo pair of 5MP monochrome machine vision cameras, a 12MP color camera for operator overlay and an NVidia Jetson Xavier NX processor. Stereo-derived point clouds are calculated within the unit itself and published over ethernet using ROS. The flexible ethernet-based architecture of WAVE allows other sensor types to be mounted.

C. Software

The WAVE testbed software is built on ROS1. The testbed implements the necessary abstractions for integration with `ros_control` [20] allowing access to the ROS ecosystem of tools including Gazebo for simulation and MoveIt! for motion planning. A set of lower-level tools also allow direct control of the testbed for manual control and diagnostics.

[1]`https://rsa-manipulation-testbed.gitlab.io/wave-documentation/`

[2]`https://trisect-perception-sensor.gitlab.io/`

Fig. 3: The Trisect underwater perception system developed by UW-APL includes two 5MP monochrome machine vision cameras for stereopsis, with a 12MP color camera for color overlay. Point clouds are calculated onboard the sensor by an NVidia Xavier NX processor and published via ROS.

D. Dynamics Simulation

A key feature of WAVE is physical embodiment of realistic dynamic coupling between the manipulator and vehicle body through passive compliance. To design a compliant pitch mechanism for the testbed, we constructed a rigid body model of an idealized Falcon ROV with a Bravo manipulator in simulation.

1) Dynamic model: The simulator was written in the Julia programming language primarily using the RigidBodyDynamics.jl library [21]. Fossen's equation is defined as [22]:

$$M\dot{\mathcal{V}} + C(\mathcal{V})\mathcal{V} + D(\mathcal{V})\mathcal{V} + g(\eta) = \tau \tag{1}$$

where $\mathcal{V}$ is the spatial velocity vector of a body in the body-fixed frame, M is the inertia matrix, $C(\mathcal{V})$ is the matrix of Coriolis and centripetal terms, $D(\mathcal{V})$ is the damping matrix, $g(\eta)$ is the vector of gravitational forces and moments (where η refers to the body's pose in the world frame) as well as buoyancy effects, and τ is the vector of control inputs and external forces. M and $C(\mathcal{V})$ both include a rigid body term (subscript RB) and an added mass term to represent the acceleration of water the vehicle displaces (subscript A): $M = M_{RB} + M_A$ and $C(\mathcal{V}) = C_{RB}(\mathcal{V}) + C_A(\mathcal{V})$. Drag on the vehicle is approximated as the summation of a linear term and a quadratic term. Drag and buoyancy forces from Fossen's equation are added as external wrenches to each manipulator link when solving the rigid body dynamics equation. Hydrodynamic parameters for the manipulator were provided by the manufacturer [19], whereas the vehicle's parameters were estimated by scaling them based on the mass of a similarly sized vehicle, summarized in [23].

Linear drag on the manipulator was ignored due to the slow velocities; otherwise, all elements included above were also applied to the manipulator. Additionally, added mass (inertia) should be direction-dependent; however, since the rigid body dynamics library does not support different inertias in different directions, added mass was simplified to be the same in each direction on each body [24].

For our use case, the vehicle was defined to be a fixed rotational joint centered at the vehicle's center of mass (COM). Gravity, buoyancy, and drag were applied as external forces, and mass is defined as the sum of actual and added mass, which is then passed to the rigid body dynamics library to simulate the motion of the system.

2) Pitch analysis: The Falcon has 2 passively stable unactuated DOF: pitch and roll. For our setup, the manipulator and perception sensor are mounted at the front of the vehicle (see Fig. 4), which shifts the system's COM forward and in turn causes the vehicle to pitch down. Since our assumption is that pitch rotation is the dominant coupling direction for precision manipulation, we restrict our analysis to manipulator motion in the XZ-plane. We will explore adding passive compliance to additional axes of the testbed in future work.

To calculate the Bravo's reachable workspace in the XZ-plane, i.e. the 'pitch plane', we sampled the space of all possible joint angle combinations (that cause motion in the plane) in 1-degree increments. For each sample, we check whether there is a self-collision or collision with the vehicle. We then used forward kinematics to calculate the end-effector position for the resulting ∼900,000 collision-free configurations (Fig. 4 shows the reachable workspace). For computational purposes, 50,000 of those manipulator configurations were uniformly sampled and passed into the Julia simulation as inputs. For each valid configuration, the simulation provides two useful data points: i) the manipulator's COM and ii) the vehicle's final pitch at equilibrium where torque applied by the manipulator's COM is balanced by buoyancy forces. We then discretized the reachable workspace into a 100x100 grid of valid configurations and averaged the final equilibrium pitch within each cell. Fig. 4 shows a workspace heatmap with the color intensity representing the final pitch over the discretized cells.

3) Compliance selection: The simulation results from Sec. III-D.2 are used to define a rotational stiffness for implementation of passive pitch dynamics in hardware. Fig. 5 plots torque from the manipulator's COM about its base τ vs. predicted vehicle pitch $\Delta\theta$. While the relationship is nonlinear, linear regression returns a reasonable approximation with an R^2 value of 0.894. The slope of the fit is the rotational stiffness:

$$k_{rotation} = \frac{\tau}{\Delta\theta} \tag{2}$$

and is found to be 1.78 $\frac{Nm}{deg}$.

Fig. 6 shows the adopted mechanical solution for reproducing the target rotational stiffness utilizing linear extension springs. The required linear stiffness was calculated with Eqn. 3

$$k_{linear} = \frac{k_{rotation}}{nr^2 cos(\theta)} \tag{3}$$

where $k_{rotation}$ is the target rotational stiffness from simulation, n is the number of linear springs, r is the height from the spring(s) anchor point, and θ is an expected pitch. Fig. 7 shows the resultant linear spring stiffnesses for varying design parameters, along with an ideal region based on the physical constraints of the testbed's vertical column. The selection of the final spring parameters was based on the expected maximum extension (due to the maximum expected pitch) and availability of off-the-shelf springs. The final parameters we chose were 2 extension springs of stiffness

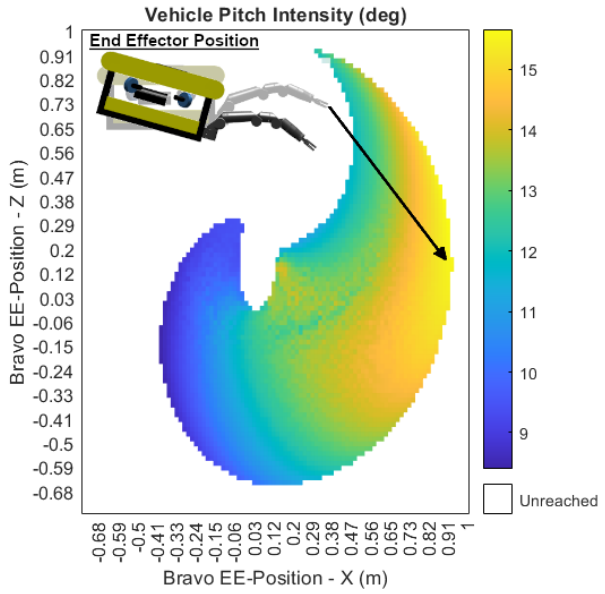

Fig. 4: Predicted UVMS pitch over the manipulator's reachable workspace. The sketch shows the final vehicle pitch for the end-effector pose indicated by the arrow.

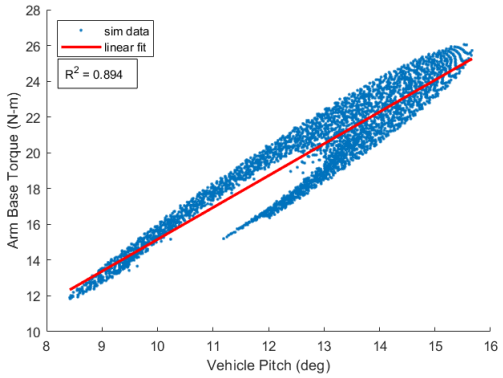

Fig. 5: Manipulator imposed torque plotted against predicted UVMS pitch with a linear fit.

132.3 $\frac{N}{m}$, a mount height of 0.6098 m, and a maximum spring extension of 0.1668 m.

E. Lab Experiments

To validate the testbed concept, we installed the system in the multi-directional wave basin at the O.H. Hinsdale Wave Research Laboratory (Corvallis, OR)[3]. The testbed was anchored to the floor and the basin was filled such that the water level was just beneath the XY frame. In addition to validating 4 controllable ROV DOF using a game controller, the primary purpose of the experiment was to compare the performance of the passive pitch mechanism against the simulated dynamics. To complete this comparison, we randomly sampled 9 target configurations from the testbed's planar XZ-workspace. We sent the manipulator to each configuration a minimum of 3 times, using an underwater string potentiometer installed at the top of the frame (see Fig. 2) to measure the frame's pitch at equilibrium. For 3 of

[3]https://engineering.oregonstate.edu/wave-lab

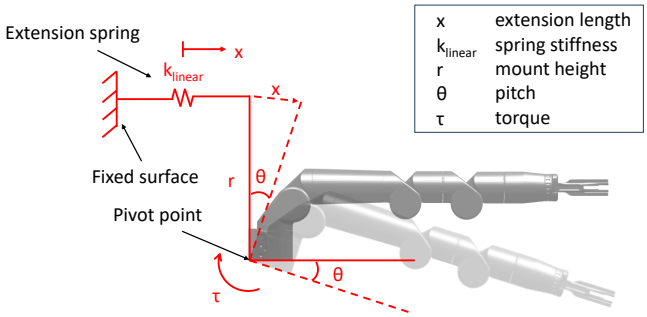

Fig. 6: Mechanical design used to replicated passive pitch dynamics on the testbed.

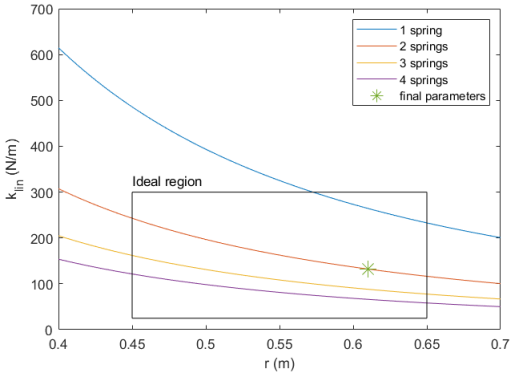

Fig. 7: Linear stiffness at varying spring mount heights for multiple springs.

the configurations, we turned on the wave generator to study how the passive dynamics behave in energetic conditions with waves of height 0.096 m at a period of 2.1 s.

IV. Results and Discussion

While installed in the Hinsdale wave basin, each of the testbed axes was successfully teleoperated through joystick control while maintaining accurate state estimation. This capability enabled other members of the research team to complete parallel studies, including data collection with the perception sensor (i.e. capturing point clouds of objects in energetic environment), a user study [25], and grasp planning experiments [26]. Each of these efforts was completed with the testbed in the locked rigid mode.

Table I shows the results of the passive pitch dynamics study where 'pred.' is the simulated equilibrium pitch and 'mean' is the average of the three measured pitches. In general, the testbed pitched approximately 3-5 degrees more than predicted by the Julia simulation. This error is most likely due to several factors, but most prominently, the use of linear extension springs is a simplification of the underlying mechanics. Additionally, there are likely modeling errors in some of the mass calculations for the components on the testbed frame, and tension from the underwater electrical cables is difficult to predict. Finally, there are some simplifying hydrodynamics assumptions in the Julia simulation, so the predicted pitches themselves may not be completely accurate. Regardless, these results show that the testbed captures some of the dynamic coupling that makes underwater manipulation challenging.

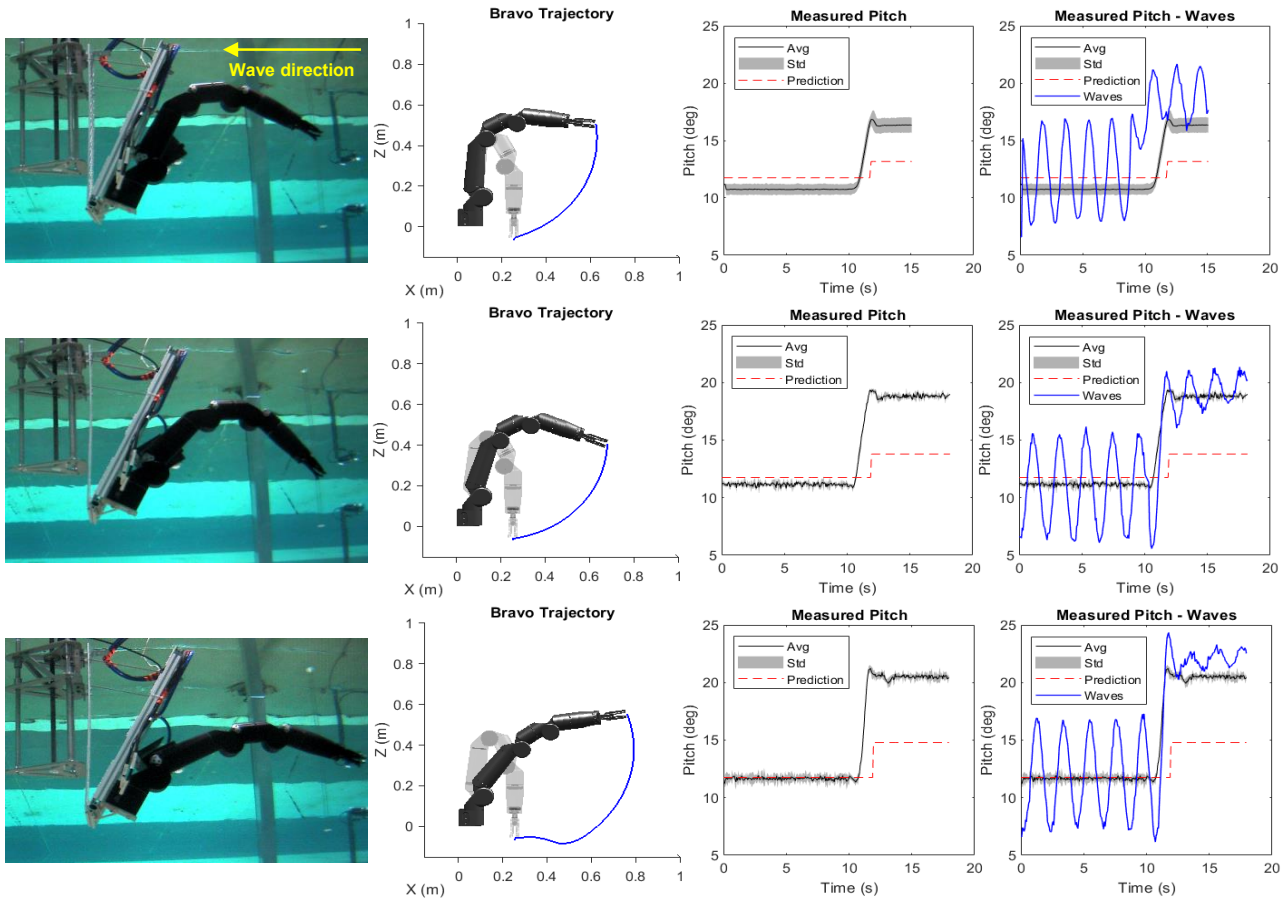

Fig. 8: *Left column*: Frame and manipulator at equilibrium (passive mode). *Left middle column*: The executed manipulator trajectory. *Right middle column*: Measured pitch after running 3 iterations of the same trajectory plotted against the predicted configuration pitch. *Right column*: Measured pitch in waves (blue) overlayed on right middle column results when waves were not running.

Fig. 8 shows images and measurements for the 3 test configurations used for wave measurements. The right most column shows the pitch measurements when the wave generator was active overlaid on the still condition measurements; here the wave height was 0.096 m and the wave period was 2.1 s. In order to use higher waves, the water level would need to be lowered to prevent splash on non-waterproof components. The testbed yaw was also oriented such that the waves were applied along the simplified x-axis towards the face of the suspended frame, direction shown in Fig. 8 (*top left*). The results show that the period of pitch oscillations matches the wave period. This may not hold true if the yaw was oriented orthogonal or even 45° to the oncoming waves. We realize that a wave basin may not be an accessible resource to the community. However, by increasing the stiffness of the springs, this proposed dynamic coupling method could be replicated in a dry lab environment. This would require the addition of mechanical damping, which the fluid provides in the underwater environment, otherwise there would likely be unrealistic oscillations around the equilibrium points.

TABLE I: Pitch compliance performance at final configuration with xz pos. representing the end-effector position and config. 0 representing the manipulator home configuration.

config.	xz pos.	pred.	mean	stdev
0	(0.252, 0.080)	11.749	11.046	0.116
1	(0.549, 0.456)	13.785	18.084	0.194
2	(0.601, 0.110)	14.531	19.037	0.125
3	(0.623, 0.536)	14.785	19.683	0.199
4	(0.680, 0.104)	14.973	19.182	0.318
5	(0.485, 0.524)	13.164	15.696	0.093
6	(0.330, 0.110)	13.913	16.507	0.180
7	(0.596, 0.170)	14.387	18.687	0.118
8	(0.516, -0.042)	14.239	19.329	0.313

V. Conclusion

In this paper, we introduce WAVE, an open-source 10-DOF kinematically redundant underwater testbed capable of partially emulating UVMS motion through a combination of controllable and passive DOFs. Through our experiments at the O.H. Hinsdale Wave Research Laborator, we demonstrated that this system is capable of maintaining accurate state estimation whilst also able to emulate a portion of a UVMS's dynamic coupling effects. While we modeled the testbed after an idealized UVMS, our system represents a platform that can be used, and iterated upon, to support future underwater manipulation studies. Future work will include the incorporation of passive roll compliance, as well as hardware upgrades to improve the overall motion and control of the testbed in energetic wave environments.

REFERENCES

[1] J. Yuh and M. West, "Underwater robotics," *Advanced Robotics*, vol. 15, no. 5, p. 609–639, Aug. 2001.

[2] B.-h. Jun, P.-m. Lee, and S. Kim, "Manipulability analysis of underwater robotic arms on rov and application to task-oriented joint configuration," *Journal of Mechanical Science and Technology*, vol. 22, no. 5, p. 887–894, May 2008.

[3] D. Cook, A. Vardy, and R. Lewis, "A survey of AUV and robot simulators for multi-vehicle operations," in *IEEE/OES Autonomous Underwater Vehicles (AUV)*, 2014, pp. 1–8.

[4] O. Matsebe, C. Kumile, and N. Tlale, "A review of virtual simulators for autonomous underwater vehicles (AUVs)," *IFAC Proceedings Volumes*, vol. 41, no. 1, pp. 31–37, 2008, 2nd IFAC Workshop on Navigation, Guidance and Control of Underwater Vehicles.

[5] J. Han and W. K. Chung, "Redundancy resolution for underwater vehicle-manipulator systems with minimizing restoring moments," in *2007 IEEE/RSJ International Conference on Intelligent Robots and Systems*, Oct 2007, p. 3522–3527.

[6] Z. Chang, Y. Zhang, Z. Zheng, L. Zhao, and K. Shen, "Dynamics simulation of grasping process of underwater vehicle-manipulator system," *Journal of Marine Science and Engineering*, vol. 9, no. 1010, p. 1131, Oct 2021.

[7] L. Gao, Y. Song, J. Gao, and Y. Chen, "Dynamic modeling and simulation an underwater vehicle manipulator system," in *2022 IEEE 9th International Conference on Underwater System Technology: Theory and Applications (USYS)*, Dec 2022, p. 1–6.

[8] M. M. M. Manhães, S. A. Scherer, M. Voss, L. R. Douat, and T. Rauschenbach, "UUV simulator: A gazebo-based package for underwater intervention and multi-robot simulation," in *OCEANS 2016 MTS/IEEE Monterey*, 2016, pp. 1–8.

[9] E. Potokar, S. Ashford, M. Kaess, and J. G. Mangelson, "Holoocean: An underwater robotics simulator," in *2022 International Conference on Robotics and Automation (ICRA)*, May 2022, p. 3040–3046.

[10] K. Cetin, H. Tugal, Y. Petillot, M. Dunnigan, L. Newbrook, and M. S. Erden, "A robotic experimental setup with a stewart platform to emulate underwater vehicle-manipulator systems," *Sensors*, vol. 22, no. 1515, p. 5827, Jan 2022.

[11] T. A. Riggs, T. Inanc, and W. Zhang, "An autonomous mobile robotics testbed: Construction, validation, and experiments," *IEEE Transactions on Control Systems Technology*, vol. 18, no. 3, p. 757–766, May 2010.

[12] S. Jatsun, O. Emelyanova, and A. S. M. Leon, "Design of an experimental test bench for a uav type convertiplane," *IOP Conference Series: Materials Science and Engineering*, vol. 714, no. 1, p. 012009, Jan 2020.

[13] A. Velasquez, N. Swenson, M. Cravetz, C. Grimm, and J. R. Davidson, "Predicting fruit-pick success using a grasp classifier trained on a physical proxy," in *2022 IEEE/RSJ International Conference on Intelligent Robots and Systems (IROS)*, Oct 2022, p. 9225–9231.

[14] K. Junge, C. Pires, and J. Hughes, "Lab2Field transfer of a robotic raspberry harvester enabled by a soft sensorized physical twin," *Communications Engineering*, vol. 2, no. 1, pp. 1–11, Jun. 2023.

[15] J.-I. Kang, H.-S. Choi, N.-D. Nguyen, J.-Y. Kim, and D.-H. Kim, "Simulation and experimental validation for dynamic stability of underwater vehicle-manipulator system," in *OCEANS 2017 - Anchorage*, Sep 2017, p. 1–5.

[16] A. Peñalver, J. Pérez, J. J. Fernández, J. Sales, P. J. Sanz, J. C. García, D. Fornas, and R. Marín, "Visually-guided manipulation techniques for robotic autonomous underwater panel interventions," *Annual Reviews in Control*, vol. 40, pp. 201–211, Jan. 2015.

[17] J. Koch, T. Pailevanian, M. Garrett, C. Yahnker, R. Detry, D. Levine, and M. Gildner, "Development of a robotic limb for underwater mobile manipulation," in *2018 OCEANS - MTS/IEEE Kobe Techno-Oceans (OTO)*, 2018, pp. 1–5.

[18] L. Christensen, P. Kampmann, M. Hildebrandt, J. Albiez, and F. Kirchner, "Hardware rov simulation facility for the evaluation of novel underwater manipulation techniques," in *OCEANS 2009-EUROPE*, 2009, pp. 1–8.

[19] R. Robotics, "Reach robotics - reach bravo," 2024, accessed: 08 Feb. 2024. [Online]. Available: https://reachrobotics.com/products/manipulators/reach-bravo/

[20] S. Chitta, E. Marder-Eppstein, W. Meeussen, V. Pradeep, A. Rodríguez Tsouroukdissian, J. Bohren, D. Coleman, B. Magyar, G. Raiola, M. Lüdtke, and E. Fernández Perdomo, "ros_control: A generic and simple control framework for ros," *The Journal of Open Source Software*, 2017. [Online]. Available: http://www.theoj.org/joss-papers/joss.00456/10.21105.joss.00456.pdf

[21] T. Koolen and contributors, "Rigidbodydynamics.jl," 2016. [Online]. Available: https://github.com/JuliaRobotics/RigidBodyDynamics.jl

[22] T. I. Fossen, *Guidance and control of ocean vehicles*. John Wiley & Sons, Ltd, 1994.

[23] J. González-García, N. A. Narcizo-Nuci, L. G. García-Valdovinos, T. Salgado-Jiménez, A. Gómez-Espinosa, E. Cuan-Urquizo, and J. A. E. Cabello, "Model-free high order sliding mode control with finite-time tracking for unmanned underwater vehicles," *Applied Sciences*, vol. 11, no. 4, p. 1836, Feb 2021.

[24] H. Kolano, E. Palmer, and J. R. Davidson, "The coupling effect: Experimental validation of the fusion of fossen and featherstone to simulate uvms dynamics in julia," Feb. 2024, arXiv:2209.13577 [cs]. [Online]. Available: http://arxiv.org/abs/2209.13577

[25] N. G. Pusalkar, M.-R. Giolando, and J. A. Adams, "Decision support system for autonomous underwater robot grasping," in *ACM/IEEE International Conference on Human-Robot Interaction*, ser. HRI '23. New York, NY, USA: Association for Computing Machinery, Mar. 2023, p. 198–202. [Online]. Available: https://doi.org/10.1145/3568294.3580071

[26] T. R. Player, D. Chang, L. Fuxin, and G. A. Hollinger, "Real-time generative grasping with spatio-temporal sparse convolution," in *IEEE International Conference on Robotics and Automation (ICRA)*. London, United Kingdom: IEEE, May 2023, p. 7981–7987. [Online]. Available: https://ieeexplore.ieee.org/document/10161529/